Review of Scientific Instruments

Simple imaging for the diamond anvil cell: Applications to hard-to-reach places

Cite as: Rev. Sci. Instrum. **89**, 103902 (2018); https://doi.org/10.1063/1.5048316
Submitted: 12 July 2018 . Accepted: 30 September 2018 . Published Online: 22 October 2018

Dean Smith, David P. Shelton, Paul B. Ellison, and Ashkan Salamat

View Online Export Citation CrossMark

ARTICLES YOU MAY BE INTERESTED IN

Contributed Review: Culet diameter and the achievable pressure of a diamond anvil cell: Implications for the upper pressure limit of a diamond anvil cell
Review of Scientific Instruments **89**, 111501 (2018); https://doi.org/10.1063/1.5049720

Fly scan apparatus for high pressure research using diamond anvil cells
Review of Scientific Instruments **90**, 015116 (2019); https://doi.org/10.1063/1.5057445

A CO_2 laser heating system for in situ high pressure-temperature experiments at HPCAT
Review of Scientific Instruments **89**, 083901 (2018); https://doi.org/10.1063/1.5040508

Lock-in Amplifiers up to 600 MHz
Watch

© 2018 Author(s).

AIP Publishing

REVIEW OF SCIENTIFIC INSTRUMENTS **89**, 103902 (2018)

Simple imaging for the diamond anvil cell: Applications to hard-to-reach places

Dean Smith,[1,a)] David P. Shelton,[2] Paul B. Ellison,[2] and Ashkan Salamat[1,a)]
[1]*Department of Physics and Astronomy and HiPSEC, University of Nevada, Las Vegas, Las Vegas, Nevada 89154, USA*
[2]*Department of Physics and Astronomy, University of Nevada, Las Vegas, Las Vegas, Nevada 89154, USA*

(Received 12 July 2018; accepted 30 September 2018; published online 22 October 2018)

The employment of high-pressure gases as a pressure-transmitting medium, sample, or reactant for diamond anvil cell experiments is widespread. As a pressure transmitter, high-pressure gases are crucial to forming quasi-hydrostatic compression atmospheres for samples inside the uniaxially driven cell. We describe an optical design for forming high-resolution images of the gasket and sample chamber of the diamond anvil cell under high gas pressures in a gas loading apparatus. Our design is simple, is of low-cost, and may be easily adapted to suit gas loading apparatus of any design, as well as other common hard-to-reach environments in diamond anvil cell experiments, i.e., those with large stand-off distances, such as cryostats. *Published by AIP Publishing.* https://doi.org/10.1063/1.5048316

I. INTRODUCTION

The hardness and incompressibility of diamond have made the diamond anvil cell (DAC) an invaluable tool for accessing extreme pressure conditions in the lab. Such a simple mechanism for applying up to millions of atmospheres of pressure—a pair of opposed diamond anvils applying uniaxial force to a sample environment—makes the DAC a highly versatile device, with geometries and materials tailored to suit desired pressure and temperature conditions, as well as required measurements.[1–5] Meanwhile, the wide transparency of diamond provides a portal for direct optical measurements to be made on samples under compression. However, the minimum working distance (WD) of optics used for measurement and imaging can be as great as 10 mm due to the thickness of the diamond anvils, the geometry of the diamond seats, and the body of the DAC itself and may still be longer due to other experimental constraints.[6] Microscope objectives used at 10 mm WD provide high resolution imaging and high numerical aperture (NA) light collection, and adequate results for WD in the range 10–50 mm can be obtained using long WD Mitutoyo objectives. However, low image resolution and light collection are obtained at the long WD imposed by the enclosure of a cryostat, vacuum furnace, or contained other environments, which may be 100 mm or longer.

One such environment with restricted optical access is the high-pressure gas loading apparatus—wherein the DAC is placed inside a vessel containing gas at pressure up to several kilobars. This approach allows samples within the DAC to be completely encapsulated in a soft pressure-transmitting medium (PTM), maintaining quasi-hydrostatic compression within the gigapascal regime despite the uniaxial nature of the device.[7] This makes high-pressure gas loading apparatus a crucial tool for the DAC community. However, the response of the gasket under load is—as expected—highly dependent on the starting density of the PTM, which then defines limits on the sample size and the maximum pressure achievable in a run. To control the loading process, it is important to be able to form images of the gasket and sample with reasonable resolution as the DAC is filled and closed inside the apparatus—a task which proves challenging when using long WD objectives placed outside of the vessel.[8–10]

Here, we report a simple, robust, and low-cost design for imaging samples in a DAC confined within the pressure vessel of a high-pressure gas loading apparatus. The basic principle of our design is the use of a short focal length lens placed close to the DAC, forming a magnified real image outside of the apparatus. Our design can be applied to gas loading apparatus of any dimensions, or if modified slightly, it can be applied to common hard-to-reach environments faced by the DAC community. Image quality is optimized by addressing chromatic and spherical aberrations, and the drastic changes in refractive indices of gas media are accounted for in the present design.

II. DESIGN OF THE APPARATUS

The DAC is placed inside the pressure vessel of the high-pressure gas loading apparatus, with steel walls several centimetres thick (Fig. 1). The gas loading apparatus was purchased from Top Industrie (Paris, France) and is capable of reaching gas pressures up to 3 kbar. Within the pressure vessel, the DAC is secured within a can and engaged with a custom-designed gearbox. A pair of hexagonal sockets on the gearbox mates with keys on the bulkhead, which is screwed down to secure a seal on the pressure vessel. These key heads may be accessed via a pair of mechanical feedthroughs, and each key turns two screws on the DAC to apply a load to the gasket and sample chamber.

The design includes a 10 mm-thick sapphire window on the underside of the pressure vessel (Fig. 1), for viewing the DAC interior during the gas loading procedure. The total distance from the diamond culets to the bottom of the pressure

a)Authors to whom correspondence should be addressed: dean@physics.unlv.edu and salamat@physics.unlv.edu

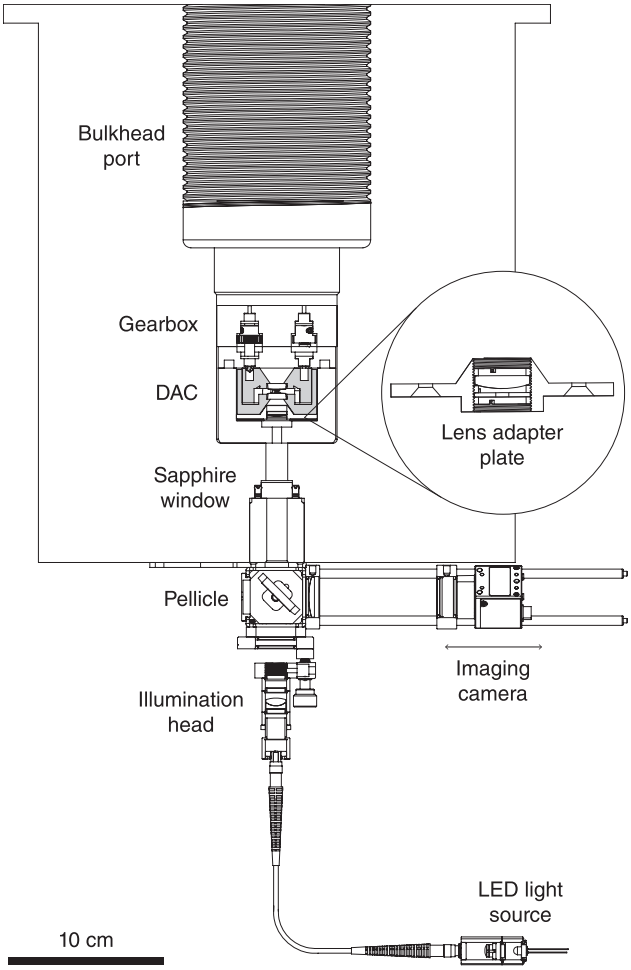

FIG. 1. A cross-sectional view of the high pressure vessel of the gas loading system, containing the gearbox with the diamond anvil cell (shaded) inside, and the imaging system attached to the underside.

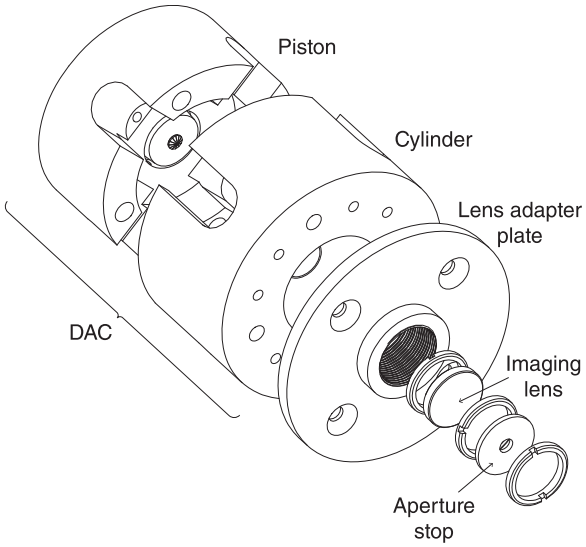

FIG. 2. Exploded view CAD model showing the imaging lens attached directly to the diamond anvil cell (DAC) via the lens adapter plate. The cylindrical nose of the lens adapter plate centers the DAC on the axis of the apparatus.

vessel is 114 mm, and the clear aperture of the optical viewing port has a diameter of 13 mm. The imaging lens is placed inside the pressure vessel, mounted directly onto the DAC (Figs. 1 inset and 2), a custom design based on that shown in Ref. 4. The lens mounting adapter reproducibly positions the lens on the rotation axis of the DAC, i.e., the line running parallel to the diamond compression axis down the center of the rotation of the cylindrical body of the DAC. The lens is held between a pair of threaded retaining rings so that the axial position of the lens can be precisely adjusted.

The design of the imaging system is shown in Fig. 3. The imaging lens (8), placed close to the DAC (9) inside the gas loading apparatus forms a magnified real image outside the gas loading apparatus where it is accessible. The present design uses a ZnSe plano-convex lens with focal length f = 13.2 mm (at λ = 633 nm). Monochromatic light is used to

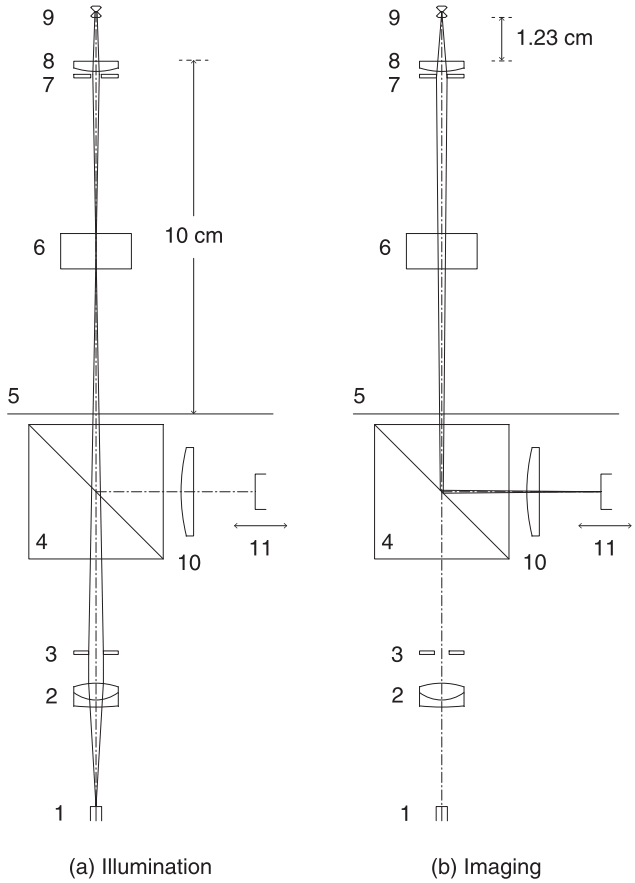

FIG. 3. Optical configuration for viewing the gasket and sample of a diamond anvil cell (DAC) placed inside the high pressure gas loading apparatus. (a) Light from optical fiber (1) is focused by lens (2) with aperture stop (3). The illumination beam assembly (1, 2, 3) is supported in an angle adjustable mount attached to the pellicle beam splitter cube (4), which is attached to the outside face of the pressure vessel (5). The light beam passes through a sapphire window (6), aperture (7), and ZnSe plano-convex lens (8), into the DAC (9). The image of fiber (1) by lens (2) is formed at or before window (6). (b) Light reflected from the DAC (9) is collected by the ZnSe lens (8) with its 3.0 mm aperture stop (7), passes through the sapphire window (6) out of the gas loading apparatus at (5), and is reflected by the pellicle (4). The reflected beam passes through plano-convex lens (10) to reach the imaging sensor surface (11) of the camera. Lens (10) is fixed on the beam splitter cube (4), and the image of the DAC (9) is brought into focus on the sensor surface (11) by moving just the camera.

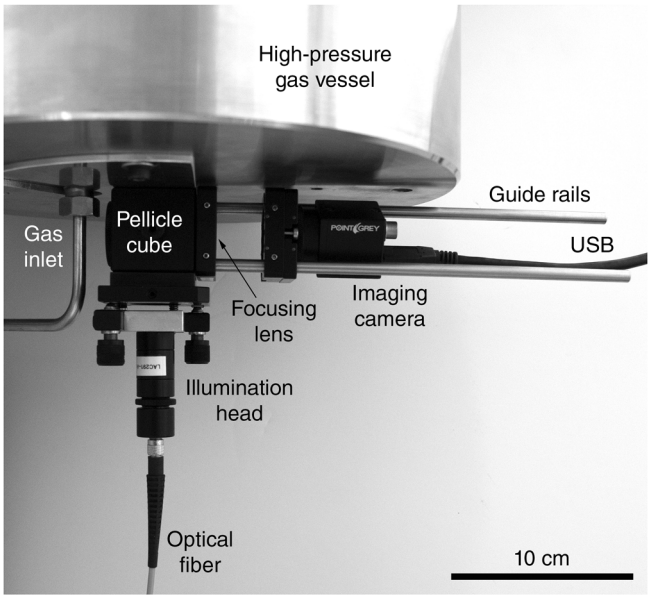

FIG. 4. Photograph showing the bottom of the pressure vessel of the high-pressure gas loading apparatus fitted with external optics.

eliminate chromatic aberration. The lens curvature and geometric aberrations are small due to the high refractive index of ZnSe ($n = 2.59$ at $\lambda = 633$ nm),[11,12] and diffraction-limited resolution $0.61\lambda/\mathrm{NA} = 3.5\ \mu$m is obtained by restricting the numerical aperture to 0.11 with the 3.0 mm diameter aperture stop (7). The ZnSe lens placed 12.3 mm from the diamond table facet (13.9 mm from the culet) forms a 14.3× magnified image 198 mm from the lens, outside the pressure vessel. The longitudinal magnification is the square of the transverse magnification, so the image position is sensitive to the lens position, with the image moving 20 mm for a 0.1 mm lens displacement.

The refractive index of He, Ne, or Ar gas at 3 kbar pressure is 1.045, 1.07, or 1.21, respectively.[13,14] The focal length of the lens increases as the refractive index of the surrounding gas increases, and a ZnSe lens was chosen since its high refractive index reduces this focal length change. For gas refractive index $n = 1.05$, the focal length increases to $f = 14$ mm and the real image formed by the lens moves to infinity, and for $n > 1.05$, the image becomes virtual. To form a real image at high gas pressure, a second lens (10) with $f = 100$ mm has been inserted

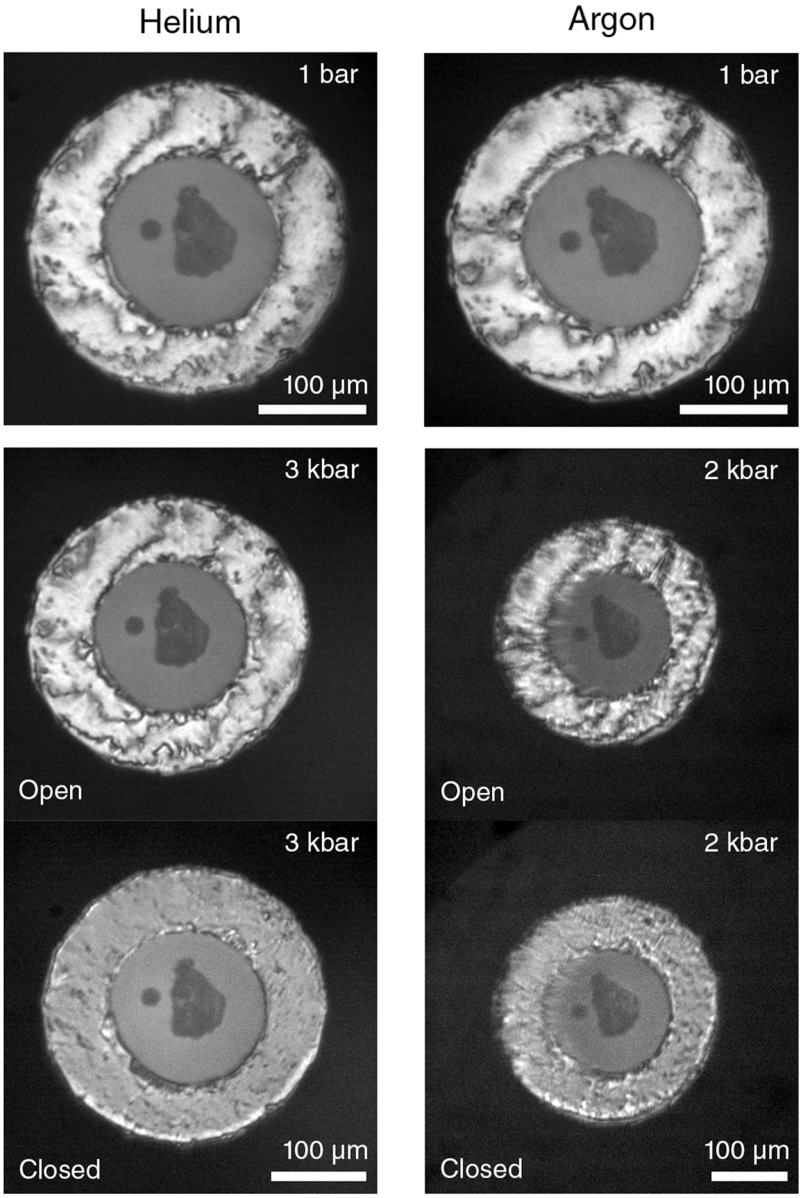

FIG. 5. Images collected *in situ* during gas loading of a diamond anvil cell equipped with 300 μm culet diamonds in a medium of (left) He to 3 kbar and (right) Ar to 2 kbar. The 180 μm sample chamber drilled into the pre-indented Re gasket by electronic discharge machining contains one chip of quartz and a small ruby sphere. Video showing closure in He is available at the link. Multimedia view: https://doi.org/10.1063/1.5048316.1

close to the ambient-pressure image plane. This lens has little effect on the low pressure image, but at high gas pressure, it continues to form a real image displaced downstream. The lens (10), fixed 58 mm before the ambient pressure image plane for the ZnSe lens, forms a final low pressure image 36 mm from the lens (10) and 176 mm from the ZnSe lens (8). For gas with n = 1.00, 1.05, or 1.20, the final image is displaced 0 mm, 65 mm, or 178 mm downstream and the final magnification is 8.4×, 7.3× or 5.8×, respectively. The image is kept in focus by translating the camera (11) along guide rails (Fig. 4).

The light source is a 5 mW red light emitting diode (LED) with spectral peak at 632 nm and spectral width 17 nm (Vishay 78-VLCS5830). The incoherent LED light has a spectrum narrow enough to show clear interference fringes at the DAC gasket and avoids the image speckle that a laser source would produce. An f = 10 mm achromatic lens couples about 5% of the LED output into the 400 μm multimode optical fiber which transports the light to the gas loading apparatus where an image of the fiber end (1) is formed inside the gas loading apparatus by the f = 25 mm achromatic lens (2). Achromatic doublet lenses are used for their lower spherical aberration.

The fiber image would be formed at the back focal plane of the ZnSe lens for the usual Kohler illumination, but if this is performed, the reflection from the sapphire window (6) will be brought to a focus close to the image plane in the camera, producing a bright spot superimposed on the desired image, and thereby reducing the image contrast or even saturating the sensor. To avoid this, the lens (2) is adjusted to form the fiber image before the window (6) so that the reflected spot from window (6) is more diffuse and less intense on the sensor (11). The divergent reflected beam from lens (8) is less of a problem. The contrast is improved by reducing the illumination beam diameter using a 4.5 mm aperture (3) so that the entire beam passes through aperture (7) and reaches the DAC. Bare sapphire and ZnSe surfaces reflect 8% and 20%, and so quarter-wavelength-thick SiO_2 anti-reflection coatings were employed to reduce the reflections to 1% per surface. This reduces the reflected light from the window and lens and increases the useful light reaching the DAC and returning to the sensor by nearly a factor of 3.

Figure 5 shows *in situ* images collected during gas loading of the same diamond anvil cell in two common pressure transmitting media—He and Ar. Interference fringes due to separation between the diamond culet and the surface of the Re gasket material are clearly defined at 1 bar and are maintained up to 3 kbar in He (n = 1.045) or 2 kbar in Ar (n = 1.18). Note that the image magnification decreases as the gas pressure and refractive index increase, and the camera is moved along its guide rails to follow the displaced image plane. Upon reaching the desired gas pressure, load is applied to the DAC via the mechanical feedthroughs until these interference fringes completely disappear—i.e., the diamonds have formed a seal on the gasket [Fig. 5 (Multimedia view) shows closure in He at 3 kbar].

III. SUMMARY AND CONCLUSION

We have developed a simple, low-cost microscope which provides diffraction-limited images of a diamond anvil cell placed 10 cm inside the chamber of a high pressure gas loading apparatus. Most notably, using this device, we are able to accurately determine closure of the diamond anvil cell whilst inside the gas loading chamber, allowing sealing of the DAC at the vessel pressure repeatably and with a 100% success rate, with typical loading times on the order of minutes. This design, with a small imaging lens fixed on the DAC, is also applicable to other experiments where the DAC is placed in an enclosure such as a cryostat which limits access to the DAC and is suitable for both transmission and reflection imaging. In fact, the design is simplified when the refractive index of the surrounding medium does not change, eliminating the need for a high-index imaging lens and an external auxilary lens. In this case, a molded glass aspheric lens or an achromatic doublet lens would be good alternatives to the ZnSe lens we have used, but the design places little constraint on the optics that can be chosen. Additionally, in principle, it would be simple to implement spectroscopy (e.g., ruby photoluminescence to measure pressure inside a DAC) to such a system, providing additional confidence in the closure of the DAC within a gas loading apparatus, or *in situ* pressure determination or sample measurements during experiments in other hard-to-reach places.

ACKNOWLEDGMENTS

The authors would like to extend thanks to Dr. Thomas Siegel of ASE Optics Europe for contributing optical design expertise for reduction of stray light in the system and assistance in assembling the optical setup. This research was sponsored in part by the National Nuclear Security Administration under the Stewardship Science Academic Alliances program through DOE Cooperative Agreement No. DE-NA0001982.

[1] L. Merrill and W. A. Bassett, Rev. Sci. Instrum. **45**, 290 (1974).
[2] R. Boehler, Rev. Sci. Instrum. **77**, 115103 (2006).
[3] D. E. Graf, R. L. Stillwell, K. M. Purcell, and S. W. Tozer, High Pressure Res. **31**, 533 (2011).
[4] I. Kantor, V. Prakapenka, A. Kantor, P. Dera, A. Kurnosov, S. Sinogeikin, N. Dubrovinskaia, and L. Dubrovinsky, Rev. Sci. Instrum. **83**, 125102 (2012).
[5] R. Boehler, M. Guthrie, J. Molaison, A. dos Santos, S. Sinogeikin, S. Machida, N. Pradhan, and C. Tulk, High Pressure Res. **33**, 546 (2013).
[6] A. Salamat, R. A. Fischer, R. Briggs, M. I. McMahon, and S. Petitgirard, Coord. Chem. Rev. **277–278**, 15 (2014).
[7] S. Klotz, J.-C. Chervin, P. Munsch, and G. L. Marchand, J. Phys. D: Appl. Phys. **42**, 075413 (2009).
[8] B. Couzinet, N. Dahan, G. Hamel, and J.-C. Chervin, High Pressure Res. **23**, 409 (2003).
[9] M. Rivers, V. Prakapenka, A. Kubo, C. Pullins, C. Holl, and S. Jacobsen, High Pressure Res. **28**, 273 (2008).
[10] A. Kurnosov, I. Kantor, T. Boffa-Ballaran, S. Lindhardt, L. Dubrovinsky, A. Kuznetsov, and B. H. Zehnder, Rev. Sci. Instrum. **79**, 045110 (2008).
[11] J. Connolly, B. diBenedetto, and R. Donadio, Proc. SPIE **0181**, 141 (1979).
[12] B. Tatian, Appl. Opt. **23**, 4477 (1984).
[13] A. Dewaele, J. H. Eggert, P. Loubeyre, and R. L. Toullec, Phys. Rev. B **67**, 094112 (2003).
[14] G. J. Hanna and M. D. McCluskey, Phys. Rev. B **81**, 132104 (2010).